



HAL
open science

Direct numerical simulation of heat transfer from liquid droplet in a continuous immiscible liquid phase

Azeddine Rachih, S. Charton, Dominique Legendre, Éric Climent

► To cite this version:

Azeddine Rachih, S. Charton, Dominique Legendre, Éric Climent. Direct numerical simulation of heat transfer from liquid droplet in a continuous immiscible liquid phase. *Congres de la Societe francaise de Thermique (SFT - 2018)*, May 2018, Pau, France. cea-02339271

HAL Id: cea-02339271

<https://cea.hal.science/cea-02339271>

Submitted on 14 Dec 2019

HAL is a multi-disciplinary open access archive for the deposit and dissemination of scientific research documents, whether they are published or not. The documents may come from teaching and research institutions in France or abroad, or from public or private research centers.

L'archive ouverte pluridisciplinaire **HAL**, est destinée au dépôt et à la diffusion de documents scientifiques de niveau recherche, publiés ou non, émanant des établissements d'enseignement et de recherche français ou étrangers, des laboratoires publics ou privés.

Direct numerical simulation of heat transfer from a liquid droplet in a continuous immiscible liquid phase

Azeddine RACHIH^{1,2*}, Sophie CHARTON¹, Dominique LEGENDRE², Eric CLIMENT²

¹ CEA, DEN, Département de recherche sur les procédés pour la Mine et le Recyclage du Combustible, SA2I, F-30207 Bagnols-sur-Cèze, France

² IMFT, Université de Toulouse, CNRS, Toulouse – France

*(Corresponding author: azeddine.rachih@imft.fr)

Abstract - Numerical simulations are used to investigate the transient, forced convection heat transfer from a spherical droplet, at low to moderate Reynolds numbers. The Navier-Stokes and heat balance equations are solved numerically in orthogonal curvilinear coordinate system, inside and outside the droplet, by a finite volume method. The results were validated against reference cases from literature. A parametric study was performed to highlight the key parameters that correlates the Nusselt number.

Nomenclature

$Z = \frac{T - T_{int}}{T_{\infty} - T_{int}}$ Dimensionless temperature

a thermal diffusivity, m^2/s

R Drop radius, m

T Temperature, K

Dimensionless numbers

Re Reynolds number

Pe Peclet number

Pr Prandtl number

Nu Nusselt number

Nu_{θ} Local Nusselt number

C_d Drag coefficient

Greek letters

λ Thermal conductivity, $W/m.K$

μ Dynamic viscosity, $Pa.s$

ν Kinematic viscosity, m^2/s

ρ Density, kg/m^3

Index and exponent

d drop phase

c continuous phase

$*$ ratio drop phase/continuous phase

1. Introduction

Heat transfer and fluid dynamics pertaining to a sphere are common in many domains. These problems belong to the class of the most fundamental subjects in fluid dynamics and heat/mass transfer that have attracted the attention of many studies [3] [4], and many applications including combustion, chemical reactions, mixing and separation processes, boiling, condensation processes In the analysis of the heat/mass transfer from spheres, three distinct configurations are usually considered [4]: the internal problem, the external problem and the conjugate problem. The first kind of problems assume that the resistance to transfer resides inside the sphere. Hence the temperature on the surface of the sphere is constant and equal to the free stream's value. The external problems consider that the thermal resistance is located outside the drop which yields a nearly uniform concentration/temperature within the droplet. No assumption can be made for the conjugate problem where the concentration/temperature is ruled by the jump conditions at the interface.

Early numerical works covering the motion inside drops include the investigation by LeClair et al. (1972) [6] who were the first to numerically study a water drop in air. Abdel-Alim and

Hamielec (1975) [8] studied liquid drops in a liquid, and Rivkind and Ryskin (1976)[9] who considered arbitrary viscosity ratios and Reynolds numbers of up to $Re = 200$. Oliver and Chung (1987) [12] verified the early numerical results and studied the fluid motion in more detail. Feng and Michaelides (2001) [5] used a method to highly resolve the boundary layer outside the sphere and simulated cases for viscosity ratios between 0 and ∞ and $Re < 1000$. Most works either studied conjugate heat/mass transfer in a low Reynolds configuration [2], or internal/external problem with intermediate or high Reynolds number [7]. Correlations of the Nusselt/Sherwood number have been developed for the later kind of problems [13] [14]. The lack of correlations in the case of conjugate transfer is the main motivation of the present study.

2. Mathematical model

2.1. Governing equations

We consider uniform flow of a Newtonian fluid past a Newtonian fluid sphere with radius R . The flows inside and outside the sphere are assumed steady and axisymmetric. The initial temperature of the drop, T_{int} , is different from that of the main stream which set to T_∞ . We consider also valid the following statements:

- the volume and shape of the drop remain constant;
- the effects of buoyancy, Marangoni convection and viscous dissipation are negligible;
- the physical properties of the sphere and the surrounding fluid are considered to be uniform, and constant;
- no emission or absorption of radiant energy;
- no phase change;
- no heat source.

The previous assumptions are usually employed in the analysis of the analogy between heat and mass transfer. Although we use only the terminology specific to heat transfer, the results are also valid for mass transfer without concentration discontinuity at the interface.

Under these assumptions, we write the mathematical model equations in a dimensionless form (the radius of the drop is considered as the characteristic length scale and the free stream velocity U_∞ as the velocity scale), over orthogonal curvilinear coordinate (ξ_j) , The parameters with a superscript "*" represent ratios of two quantities where the numerator is the drop phase parameter while the denominator parameter corresponds to the continuous phase.

In a general curvilinear orthogonal coordinates (ξ_i) , the Navier–Stokes and the continuity equations, read

$$\begin{aligned} \frac{\partial V_j^\delta}{\partial \xi_j} &= 0 \\ \frac{\partial V_i^\delta}{\partial t} + \frac{\partial (V_i^\delta V_j^\delta)}{\partial \xi_j} &= -\frac{\partial P^\delta}{\partial \xi_i} + \frac{\partial (\tau_{ij}^\delta)}{\partial \xi_j} + H_j^i (V_j^\delta V_j^\delta - \tau_{jj}^\delta) - H_j^i (V_i^\delta V_j^\delta - \tau_{ij}^\delta) \end{aligned} \quad (1)$$

Where the superscript δ stands for the phase ($\delta = d$ (inside the drop) or $\delta = c$ (for the external phase)). V_j^δ being the dimensionless velocity field in the phase δ , τ_{ij}^δ represents the components of the dimensionless viscous stress given by :

$$\begin{aligned}\tau_{ij}^d &= \frac{1}{Re} \left[\frac{\partial V_i^d}{\partial t} + \frac{\partial V_j^d}{\partial V_i^d} - H_j^i V_j^d - H_i^j V_i^d + 2H_i^k V_k^d \delta_{i,j} \right] \\ \tau_{ij}^c &= \frac{\mu^*}{Re} \left[\frac{\partial V_i^c}{\partial t} + \frac{\partial V_j^c}{\partial V_i^c} - H_j^i V_j^c - H_i^j V_i^c + 2H_i^k V_k^c \delta_{i,j} \right]\end{aligned}\quad (2)$$

H_j^i is the curvature factor given in terms of the factor scale h_i along the direction i , as $H_j^i = \frac{1}{h_j} \frac{\partial h_j}{\partial \xi_i}$. The Reynolds number shown in the τ_{ij}^δ expression writes $Re = \frac{2U_\infty R}{\nu^c}$. As there is no heat source, the following dimensionless heat transport equation involves only diffusive and convective transports. In the considered coordinate system (ξ_i) it writes :

$$\begin{array}{cc}\text{Drop phase} & \text{Continuous phase} \\ \frac{\partial Z^d}{\partial t} + \frac{\partial (V_j^d Z^d)}{\partial \xi_j} = \frac{1}{Pe} \frac{\partial^2 Z^d}{\partial \xi_j \partial \xi_j} & \frac{\partial Z^c}{\partial t} + \frac{\partial (V_j^c Z^c)}{\partial \xi_j} = \frac{a^*}{Pe} \frac{\partial^2 Z^c}{\partial \xi_j \partial \xi_j}\end{array}\quad (3)$$

Z is the dimensionless temperature (i.e. $Z = \frac{T - T_{int}}{T_\infty - T_{int}}$), and $Pe = \frac{2U_\infty R}{a^c}$ is the external Peclet number. Note that the Peclet can be calculated from the Reynolds number and the Prandtl number $Pr = \frac{\nu^c}{a^c}$.

In order to couple the internal and the external flows, one must complete the previous set of equations by the jump conditions expressed at the interface. At the droplet interface ($r = R$), which is considered completely free from any surface-active contaminants, it is assumed, that the component of the shear stress tangent to the interface is continuous across the interface. The balance of the component of the shear stress normal to the interface is unnecessary since the interface is considered as non-deformable and spherical. In addition, it is assumed that the component of the velocity tangent to the interface is continuous across the interface, and that the component of the velocity normal to the interface equals zero in both phases. Finally the temperature and the normal local heat flux are continuous at the interface. Therefore, the jump conditions can be summarized in the following equations :

$$\begin{aligned}\mathbf{V}^d \cdot \mathbf{t} &= \mathbf{V}^c \cdot \mathbf{t} \\ \mathbf{V}^d \cdot \mathbf{n} &= \mathbf{V}^c \cdot \mathbf{n} = 0 \\ (\boldsymbol{\tau}_I^d \cdot \mathbf{n}) \cdot \mathbf{t} &= (\boldsymbol{\tau}_I^c \cdot \mathbf{n}) \cdot \mathbf{t} \\ Z_I^d &= Z_I^c \\ -\lambda^d \frac{\partial Z^d}{\partial \mathbf{n}} \Big|_I &= -\lambda^c \frac{\partial Z^c}{\partial \mathbf{n}} \Big|_I\end{aligned}\quad (4)$$

3. Results & Discussion

3.1. Numerical procedure

The previous balance equations of the model are solved numerically using the code JADIM. This inhouse research code, developed by IMFT [10] [11], uses the finite volume method to solve the 3D unsteady and incompressible Navier–Stokes equations in orthogonal curvilinear coordinates. A 2D axisymmetric geometry has been used in our study. The mesh used for the computational domain is a curvilinear orthogonal mesh where the internal mesh is polar and the external one represents the stream/potential functions of an inviscid flow around a cylinder (Figure 1).

The algorithm of resolution relies on the projection method, where the diffusive-convective terms are evaluated first. Then the pressure is computed to satisfy the incompressibility condition through the solution of a Poisson equation. The numerical scheme of time advancement based on Range-Kutta/Crank-Nicholson presents an efficient stability with a second order. The viscous terms are calculated implicitly while the convective terms are solved explicitly. The spatial discretization is based on a centered scheme (second order). The resolution of pressure is run independently inside and outside the droplet.

The hydrodynamics problem is solved for a given Re number until a steady state is reached. The energy equation is then resolved subsequently in the frozen velocity field with an initial value of $Z_0^d = 1$ inside the droplet and 0 everywhere outside.

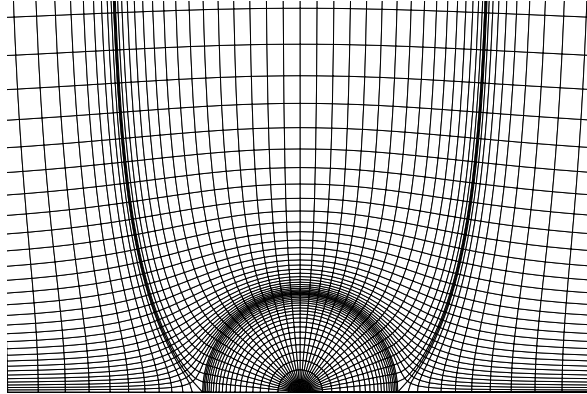


Figure 1: Curvilinear orthogonal mesh used in the simulations

3.2. Validations

Two key parameters have been investigated to test the accuracy of our numerical model: the drag coefficient C_d , for the hydrodynamic aspect, and the Nusselt number for the heat transfer aspect. The drag coefficient is calculated from the total drag force F_D exerted by the continuous phase on the droplet, using the classical definition $C_D = 8 \frac{F_{D,p} + F_{D,f}}{\pi \rho^e U_\infty^2 d^2}$. This drag force is calculated by the shell integration of the x-component of the viscous stress and pressure on the droplet interface. The Nusselt number is defined by the expression :

$$Nu = \frac{1}{T^d} \int_{drop} \left. \frac{\partial T^d}{\partial \mathbf{n}} \right|_I \cdot \sin(\theta) dS \quad (5)$$

$\overline{T^d}$ is the average temperature inside the droplet, given as follows :

$$\overline{T^d} = \frac{3}{4\pi R^3} \int_0^{2\pi} \int_0^R \int_0^\pi T^d(r, \theta) r^2 \sin(\theta) dr d\theta d\Omega \quad (6)$$

The numerical results are first compared with literature correlations for the drag coefficient. The results are summarized in Table 1. The calculated drag coefficients are in excellent agreement with the literature data in the considered range of Reynolds number used. If we look at the streamlines pattern of the case ($Re = 100, \rho^* = 1$) shown in Figure 2, we can notice an external recirculation in the wake of the drop. The same external recirculation was observed by Oliver & Chang (1987), the angle at which the boundary layer separates was found by the authors to be 41.1. In our results the value found is 41.7 which is in very good agreement.

| Re | 0.1 | 0.5 | 1 | 2 |
|-----------------------|-------|-------|-------|------|
| Present simulations | 205.3 | 42.89 | 22.5 | 12.1 |
| Oliver & Chung [12] | 202.4 | - | 22.4 | 12.1 |
| Feng & Michalides [5] | - | 42.61 | 22.42 | - |

Table 1: Drag coefficient ($\rho^* = 1$)

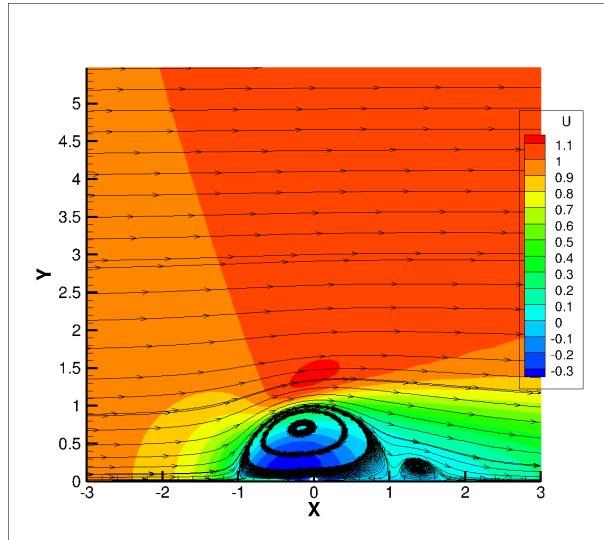


Figure 2: Distribution of the horizontal velocity and streamlines ($Re = 100, \rho^* = 1$)

Figure 3 compares the time evolution of the Nusslet number, predicted by our simulation with data from Oliver and Chung [2] for droplets in the creeping flow regime ($Re = 0.1$). The overall agreement is good and especially the temporal oscillations due to the convection process inside the droplet are correctly reproduced. It is worth to note that the magnitude of the oscillations depends primarily on the Peclet number. Hence, for low Peclet number the transport process is diffusive and the effect of the internal recirculation cannot be seen. As as the Pe increases the internal recirculation triggers oscillations of the Nusselt number, before reaching steady state. Again, the steady values are in perfect agreement with [2] as reported in

| Pe | 50 | 100 | 200 | 500 | 1000 |
|----------------------|------|-----|-----|------|------|
| Present calculations | 2.72 | 3.6 | 4.8 | 7.19 | 9.14 |
| Olivier & Chung [2] | 2.67 | 3.6 | 4.8 | 7.2 | 9.2 |

Table 2: Steady values of the Nusselt number ($Re = 1$, $\mu^* = 1$, $a^* = 1$)

Table 2 for an internal problem where the stream flow imposes its temperature on the droplet's interface. The time evolution of the local Nusselt number profiles in a creeping flow ($Re = 0.1$) is compared with Juncu's result [7] in Figure 4. An excellent agreement is observed for the spacial distribution of local Nusselt number evolution.

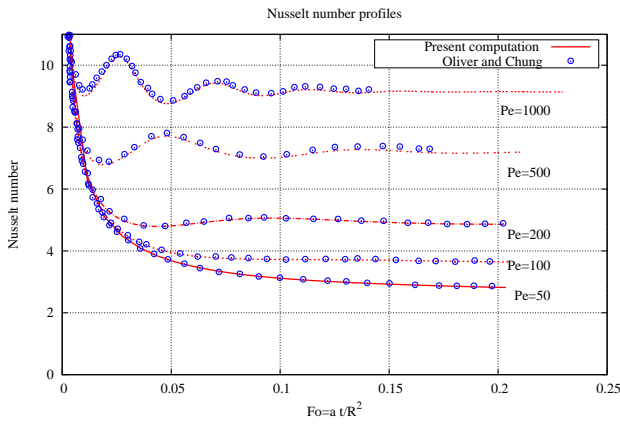


Figure 3: Temporal evolution of Nusselt number ($Re = 0.1$)

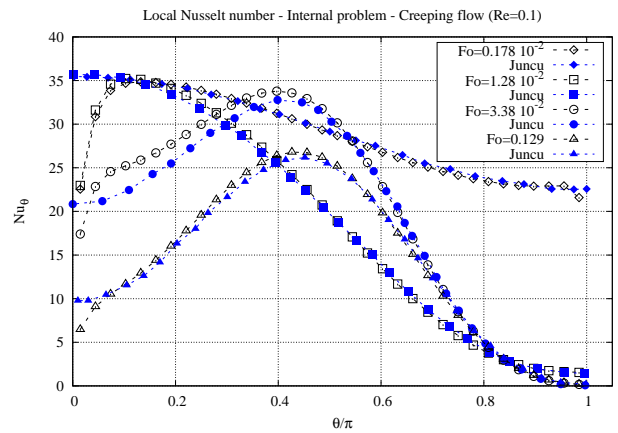


Figure 4: Temporal evolution of Nu_θ profiles ($Re = 0.1$, $Pe = 1000$)

3.3. Parametric study

In order to identify the key parameters that drive the variation of the Nusselt number, we perform a parametric study by varying the dimensionless number one by one. Among the three parameters representing to hydrodynamics (Re , μ^* and ρ^*), studies[5] [15] have shown that the density ratio effect is small in axisymmetric problems therefore we reduce our hydrodynamic parameters to the Reynolds number and the viscosity ratio, (the density ratio bring fixed to 1). Similarly the parameters that influence the physics of the transfer are the Peclet number and the thermal diffusivity ratio. To investigate these parameters we start by studying the evolution of the Nusselt number in terms of Peclet number for a given hydrodynamic configuration. Figures 5 and 6 correspond to two different flow regimes ($Re = 0.1$ and $Re = 100$). In those figures, the yellow regions represent curves with $a^* > 1$ while the pink regions are associated with $a^* < 1$. It can be noticed that the two cases show similar tendencies regarding the Nusslet evolution, however a significant effect of μ^* and a^* can be noticed. The absence of similarities and the multi-variable aspects make it very difficult to predict a correlation for Nu . One way to use efficiently the data is by studying limiting cases. Future work will shed light on this strategy.

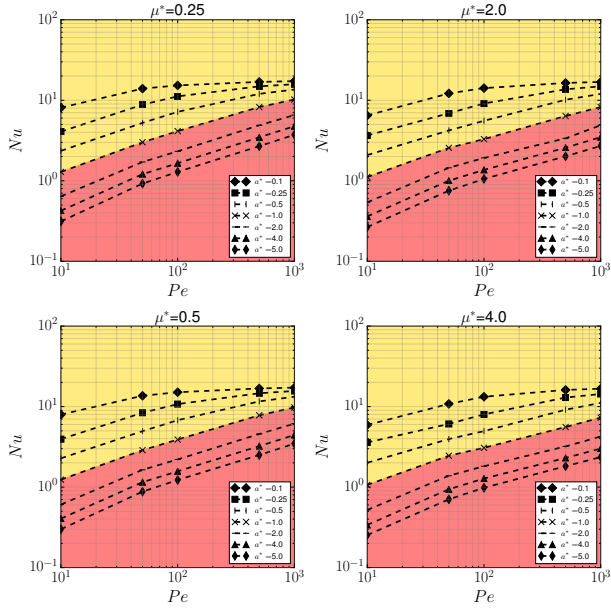


Figure 5: Nusselt number $Re = 0.1$

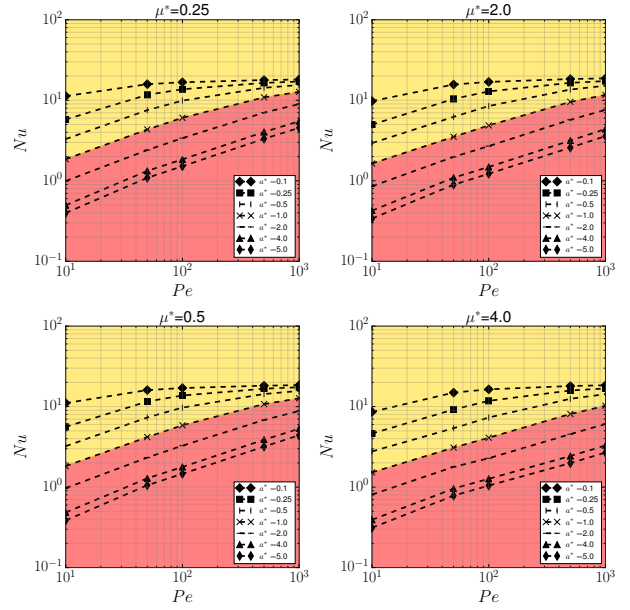


Figure 6: Nusselt number $Re = 100$

4. Conclusion

In this contribution, we have carried out simulations that resolves Navier-Stokes equations and heat transport equation inside and outside a spherical droplet. Jump conditions at the interface have been implemented to couple the internal/external flows. The hydrodynamic validation has been performed for a wide range of Re . For heat transfer, the Nusslet number evolution has been validated for low Reynolds flows. The number of parameters controlling the heat transfer rate may vary from one case to another: the conjugate problem depends on a large number of parameters which makes it difficult to derive a direct correlation from the simulation's results. One way to investigate the problem will be to study extreme cases (1- Internal/external problem which corresponds respectively to large/small values of diffusivity ratio or 2- Particle/bubble characterized by extreme values of viscosity ratio).

5. Bibliography

References

- [1] Juncu, Gheorghe, A numerical study of the unsteady heat/mass transfer inside a circulating sphere, *International Journal of Heat and Mass Transfer*, 53, 15, 3006–3012, 2010
- [2] Oliver, Douglas LR and Chung, Jacob N, Conjugate unsteady heat transfer from a spherical droplet at low Reynolds numbers, *International journal of heat and mass transfer*, 29, 6, 879–887, 1986
- [3] Clift, R and Grace, JR and Weber, ME, Bubbles, drops and particles, 1987, Book
- [4] Sadhal, Satwindar S and Ayyaswamy, Portonovo S and Chung, Jacob N, Transport phenomena with drops and bubbles, 2012 Book
- [5] Feng, Zhi-Gang and Michaelides, Efstathios E, Drag coefficients of viscous spheres at intermediate and high Reynolds numbers, *Transactions-American Society Of Mechanical Engineers Journal Of Fluids Engineering*, 123, 4, 841–849, 2001
- [6] LeClair, B.P., Hamielec, A.E., Pruppacher, H.R., Hall, W.D., A theoretical and experimental study of the internal circulation in water drops falling at terminal velocity in air, *J. Atmos. Sci.*, 29 (4), 728–740, 1972
- [7] Juncu, Gheorghe, A numerical study of the unsteady heat/mass transfer inside a circulating sphere, *International Journal of Heat and Mass Transfer*, 53, 15, 3006–3012, 2010
- [8] Abdel-Alim, A.H., Hamielec, A.E., A theoretical and experimental investigation of the effect of internal circulation on the drag of spherical droplets falling at terminal velocity in liquid media, *Industr. Eng. Chem. Fundam.*, 1975, 14 (4), 308–312
- [9] Rivkind, V.Y., Ryskin, G.M., Flow structure in motion of a spherical drop in a fluid medium at intermediate Reynolds numbers, *Fluid Dyn.*, 53, 15, 11 (1), 5–12, 1976
- [10] Legendre, Dominique, Quelques aspects des forces hydrodynamiques et des transferts de chaleur sur une bulle sphérique, 1996 - Thèse de l'INP Toulouse
- [11] Claire Souilliez, Hydrodynamique d'une goutte sphérique, 2004 - Rapport de stage DEA, IMFT
- [12] Oliver, DLR and Chung, JN, Flow about a fluid sphere at low to moderate Reynolds numbers, *Journal of Fluid Mechanics*, 177, 1–18, 1987
- [13] Kumar, A and Hartland, S, Correlations for prediction of mass transfer coefficients in single drop systems and liquid–liquid extraction columns, *Chemical Engineering Research and Design*, 77, 5, 372–384, 1999
- [14] Wegener, M and Paul, N and Kraume, M, Fluid dynamics and mass transfer at single droplets in liquid/liquid systems, *International Journal of Heat and Mass Transfer*, 71, 475–495, 2014
- [15] Edelman, Christopher A and Le Clercq, Patrick C and Noll, Berthold, Numerical investigation of different modes of internal circulation in spherical drops: Fluid dynamics and mass/heat transfer, *International Journal of Multiphase Flow*, 95, 54–70, 2017

Acknowledgements

This work was supported by the Nuclear Energy Division of CEA (program SIACY). The authors acknowledge the COSINUS service at the IMFT for their technical support: Kevin LARNIER, Annaïg PEDRONO.